2024 IEEE International Conference on Robotics and Automation (ICRA 2024)
May 13-17, 2024. Yokohama, Japan

Design & Systematic Evaluation of Power Transmission Efficiency of an Ankle Exoskeleton for Walking Post-Stroke

Myles Cooper[1,†], Santiago Canete[1,†], Asa Eckert-Erdheim[1], Aidan Kimberley[1]
Christopher Siviy[1], Teresa Baker[2], Terry D. Ellis[2], Patrick Slade[1], Conor J. Walsh[1,*]

***Abstract*— Community-based locomotor training post-stroke has shown improvements in independent ambulation by increasing dose, intensity, and specificity of walking practice. Robotic ankle exoskeletons hold the potential to facilitate continued rehabilitation at home, but understanding what aspects of the design are most relevant for successful translation to the community presents a challenge. Here, we design a portable rigid ankle exoskeleton to use as a research platform for investigating the effect of assistance on post-stroke gait during overground, community-based walking. We first test our device with stroke survivors and validate its potential for future community use. We then present a systematic method for quantifying power transmission losses at each transmission stage from the battery to the wearer, using data gathered from walking trials with healthy participants. Our evaluation method revealed inefficiencies in power transfer at the interface level, likely resulting from the compliance in the structural components of the system, which motivates future redesign considerations. Overall, our method provides a framework to identify and characterize the components that must be redesigned to lower exoskeleton weight and maximize performance.**

I. INTRODUCTION

Mobility recovery post-stroke tends to plateau within three to five months, after which stroke survivors are discharged from in-patient therapy. Patients are often left with lifelong walking deficits [1] that can limit community engagement and reduce quality of life [2]. Continuing community-based locomotor training has shown improvements in independent ambulation by increasing dose, intensity, and specificity [3], [4]. However, traditional rehabilitation interventions that rely heavily on physical therapists can be challenging to continue long-term through outpatient care. Thus, research into alternative methods that allow patients to continue rehabilitation in community settings is critical to improving mobility outcomes post-stroke.

Robotic ankle exoskeletons have the potential to assist during post-stroke rehabilitation interventions. By assisting the paretic ankle, exoskeletons can increase foot clearance during the swing phase [5], [6], [7] and improve forward propulsion during push-off [8], [5], reducing the use of inefficient compensation strategies like hip circumduction and hip hiking [8]. However, most successful devices have been limited to the clinic. Continuing rehabilitation with an exoskeleton at home could help increase forward propulsion and daily step count, [9] which could lead to greater community engagement. Although this initial work has shown promising results, further research into the long-term effects of using exoskeletons during at-home rehabilitation is necessary to address the high variability in outcomes across participants.

Prototyping new portable devices to be used by stroke survivors in the community can help us understand device usability (e.g. donnability, weight) and performance (e.g. control accuracy, efficiency) outside the laboratory. In this way, we can investigate the relative contribution of these design elements to overall device effectiveness in realistic settings, allowing us to identify what distinguishes stroke survivors who benefit from assistance and those who do not. Furthermore, portable prototypes can provide a suitable research platform for controller design and optimization in a community setting [10], where the variability of walking differs substantially from inside the laboratory. Overall, through human-in-the-loop development and community pilots with end users, we can learn how interface, actuation, and controller design collectively impact the user. This understanding can ultimately help optimize the human-robot interface to position the technology for translation to the community.

When designing a portable ankle exoskeleton, balancing the tradeoffs between device performance and impact on the user presents a challenge. For healthy populations, higher levels of torque at the ankle joint increase the energetic benefits of assistance [11], [12], [13]. However, increasing the power output of an exoskeleton requires increasing the size and weight of the motor and battery, which may have a negative effect on energetic cost [14]. While for healthy populations the tradeoffs between assistance magnitude and weight have been well studied, we do not yet understand what levels of assistance are needed to consistently benefit users post-stroke. Previous work has shown that lightweight exosuits can help users' post-stroke walk for longer periods of time while improving clinically relevant gait metrics [15], [16]. Thus, initial prototypes for community-based rehabilitation post-stroke should aim to minimize device weight while providing a range of assistance capabilities

This work was supported by the Eunice Kennedy Shriver National Institute Of Child Health & Human Development of the National Institutes of Health Award BRG-R01HD088619. The content is solely the responsibility of the authors and does not necessarily represent the official views of the National Institutes of Health. This work is also supported by the National Science Foundation Award CMMI-1925085, and the Harvard University John A. Paulson School of Engineering and Applied Sciences.

This work involved human subjects or animals in its research. Approval of all ethical and experimental procedures and protocols was granted by Harvard Medical School Institutional Review Board.

†: M. Cooper and S. Canete contributed equally to this work

*: Corresponding author: walsh@seas.harvard.edu

1: Harvard John A. Paulson School of Engineering and Applied Sciences, Boston, MA, USA.

2: Department of Physical Therapy and Athletic Training, Boston University, Boston, MA, USA.

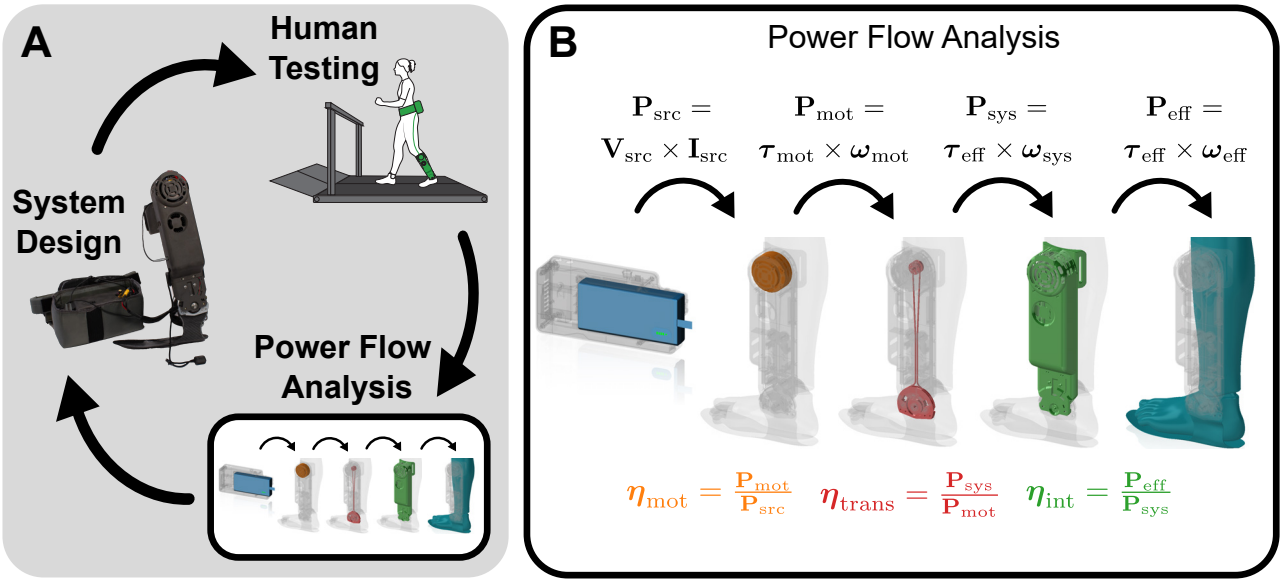

Fig. 1. A) Proposed design and evaluation paradigm: we design a portable rigid ankle exoskeleton to be used as a research platform for investigating the effect of assistance on post-stroke gait. We perform preliminary tests with stroke survivors walking overground, and based on the results obtained we present a systematic method for quantifying power transmission losses at each stage of the transmission. Then, we identify aspects of our design that can be improved to increase efficiency and lower overall weight and we repeat in an iterative process. B) Proposed benchtop evaluation paradigm: we measure power flow through the system at multiple stages by replaying data from human subjects testing on a benchtop dynamometer. We then calculate efficiencies for each component of the device by taking the ratios of those powers through time.

that facilitate research into control requirements. Designers must understand how each component of the system affects the power transfer from the battery to the wearer's biological joint to design exoskeletons that can deliver assistive power effectively while minimizing their encumbrance to the wearer.

The ability to identify the relative contribution to transmission efficiency from each component of the exoskeleton will help designers model, improve, and validate the design in a systematic, iterative process. Existing studies that have evaluated the power efficiency of exoskeletons are highly heterogeneous and often have been performed in testing conditions that are not representative of real-world use. Research groups have presented overall power transmission efficiencies[17], [18] or bandwidth measurements [19] of various devices. However, these studies do not quantify the specific contributors to performance limitations, making it difficult to use these results to improve upon previous designs.

The objective of this study was to develop an initial portable, self-donnable, rigid ankle exoskeleton research platform for investigating the potential to assist post-stroke gait during overground, community-based walking. We outline the design and validation process, incorporating considerations specific to stroke survivors walking in a community setting, such as bidirectional assistance for ground clearance and propulsion; simple closures and a full-length foot plate for ease of donning; and portability. Based on the preliminary results obtained from initial overground walking tests with stroke survivors, we present a systematic method for quantifying power losses at each stage of the transmission from the battery to the wearer (Fig. 1). This method allows us to identify the specific aspects of our design that can be improved to increase efficiency and lower overall weight by characterizing performance in conditions that better resemble real-world use. This method quantifies the different contributors to performance loss, thus we believe it could be used as a systematic tool for exoskeleton development.

II. Exoskeleton Design & Validation

A. Overview

The unilateral ankle exoskeleton used in this paper consists of a distal actuation system and a waist pack containing the controller and battery (Fig. 2). The assistance characteristics are targeted at post-stroke populations that can benefit from bidirectional assistance in both plantarflexion (PF) and dorsiflexion (DF). We chose to target a 30° range of motion in DF and a maximum assistance torque in PF of 30 N*m based on a previous community-based ankle exoskeleton targeting post-stroke walking [9].

B. Mechanical Design

1) Ankle Mechanism and Actuation System: We chose to use a low gear ratio, distally-mounted motor to circumvent the inefficiencies associated with high-ratio gearboxes and long Bowden cables [20], as we predicted that the improved back drivability and overall system efficiency would compensate for the added distal mass. The distal actuation system of the exoskeleton is composed of a high torque-density brushless DC motor (AK60-6 V1.1, Cubemars, China) with a quasi-direct drive transmission (6:1 planetary gear), and then geared by another 5.2:1 ratio using aluminum pulleys

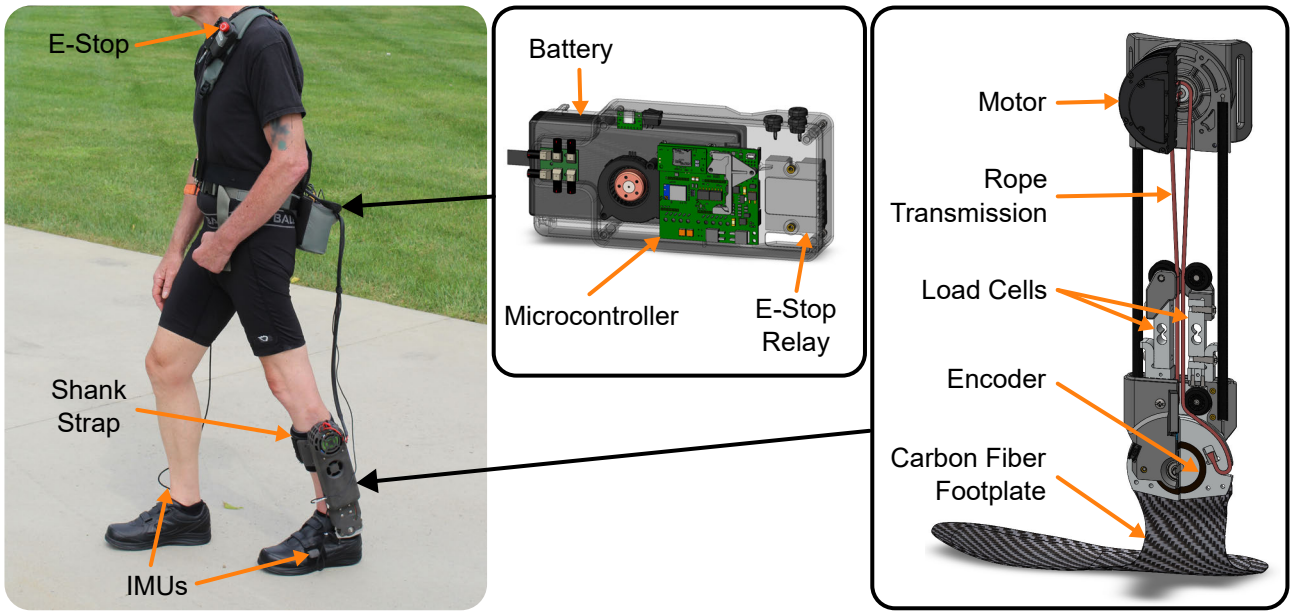

Fig. 2. On the left, the device worn by a person post-stroke: waist pack, exoskeleton on the paretic side, and IMU sensors. On the right, the waist pack diagram shows onboard custom electronics and the exoskeleton with sensors, transmission, and footplate. The exoskeleton design is targeted at assisting users post-stroke and thus features a full footplate, bidirectional assistance, and distal actuation for higher efficiency and lower weight.

connected by a 3 mm diameter rope (Vectran, Kuraray Co., Japan).

The motor and pulley transmission apply a torque about a pin joint aligned with the ankle joint, transferred to the shank through a plastic-reinforced webbing strap, and transferred to the foot through a carbon fiber footplate inserted into the shoe. The footplate extends from the heel to the toe of the wearer's shoe and was custom-made using eight layers of 6k 2x2 twill fiber (H2550 C10, Hyosung, Korea), which tapers to four layers just proximal to the metatarsophalangeal joint to allow the toes to bend naturally.

2) Waist Pack: The waist pack contains the controller electronics composed of a custom board using an Atmel processor (SAME70N21, Atmel Co., USA) and running a custom Real-Time Operating System. The communication between the board, sensors, and motor control unit (MCU) happens through CAN protocol. The waist pack houses a 25.2 V, 3.9 Ah Lithium Ion Battery (RRC3570, RRC Power Solutions, Germany), which supplies power through a solid-state relay attached to a handheld emergency stop button.

The waist pack attaches to the wearer with a belt and shoulder strap that can be adjusted to a wide range of wearer heights and widths. The shoulder strap also features cable tie-downs and a pocket that holds an emergency stop button and a handle that can toggle the exoskeleton between active and inactive states.

3) Sensing: The actuation system monitors actuator torque by summing the loads measured by two cantilever load cells (3133_0, Phidgets, Canada) that measure cable tension using the reaction force applied by bending the rope around a pulley. The load cells were calibrated on a custom dynamometer (see section III-C.1) to correlate with the torque at the ankle. The angle of the actuator is measured with an off-axis hall effect encoder (Lamprey2, Team 221 LLC., USA). One inertial measurement unit (IMU) (MTi-3, XSens, Netherlands) is worn on each shoe to monitor sagittal foot-to-floor angle for use in gait detection.

C. Event Detection & Control

1) Gait Segmentation: The gait segmentation algorithm has been validated and described in previous work by our group [5]. Briefly, our method detects paretic and nonparetic toe-off events and nonparetic mid-swing based on the sagittal plane nonparetic foot IMU measurements. This is done by detecting negative peaks in the sagittal plane foot angular velocity during walking. Using these discrete events, the gait cycle can be segmented into three phases: paretic mid-stance, paretic terminal stance, and paretic swing. This method is suitable for gait phase detection in users with variable gaits (e.g., stroke survivors).

2) High-level Controller: During paretic support, the controller generates a desired PF torque profile that consists of two cubic splines, one rising and one falling, based on the desired onset, peak, and offset timing of assistance, as well as peak magnitude. The timing of the profile is based on percent paretic support (%PS) as described in previous work [5]. During the paretic swing phase, the device transitions to a position controller that commands a desired DF angle.

3) Low-level Controller: The motor is controlled in velocity mode and the desired position and torque are mapped to motor velocity commands via an admittance controller with a proportional gain and a damping injection term acting on motor velocity (measured by the internal encoder on the motor) as detailed by Zhang et al. [21].

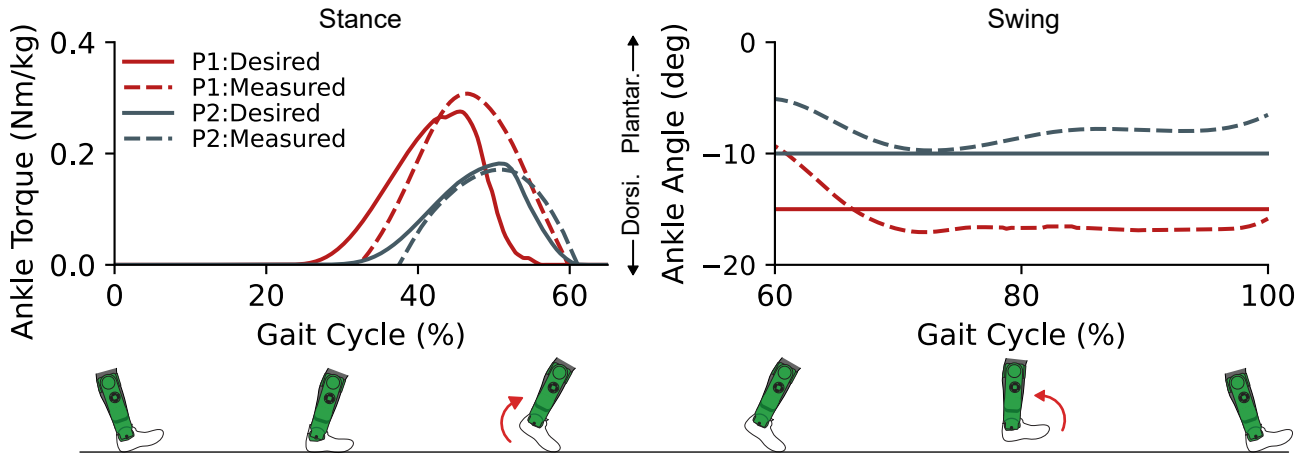

Fig. 3. Mean desired and measured ankle torque during stance and ankle angle during swing for 2 stroke survivors (P1, P2) walking with an ankle exoskeleton overground. We identify tracking errors in ankle torque RMSE: 0.14±0.04 N*m/kg and in ankle angle RMSE: 2.14±0.13°. Based on these results we propose a systematic evaluation method that allows us to identify the key aspects of the design that could be improved for achieving higher efficiencies in power transmission.

D. Testing with Stroke Survivors

1) Protocol: To validate the usability of the device for post-stroke community use, we recruited two stroke survivors with prior experience using a soft ankle exosuit. We tracked their movement using motion capture cameras (sample rate: 200 Hz; Qualisys, Göteborg, Sweden) and reflective markers. We measured ground reaction forces using a set of 9 force plates installed on the ground (sample rate: 1200 Hz; Bertec, Ohio, USA). The two participants performed 10 passes for each condition (1: with regular shoes, 2: exoskeleton powered) of overground walking on the instrumented indoor track. Both participants were given ∼5 minutes to acclimate to the device prior to the collection, during which, assistance profiles at the ankle were tuned to their comfort. The assistance profiles were computed using a quintic spline and determined by peak torque, peak timing, onset timing, and offset timing [11], [12], [13]. One participant completed an outdoor walking trial that consisted of level walking on the sidewalk to validate the usability of the device outside of the laboratory. Additionally, both participants were instructed on how to don the system independently and timed to inform future designs for at-home use.

2) Performance Validation & Usability for Users Post-Stroke: While the device was able to apply the commanded torques and positions throughout gait, torque assistance was delayed by an average of 0.35% gait cycle, with a root mean square (RMS) error of 0.14±0.04 N*m/kg, and dorsiflexion angle assistance had an RMS error of 2.14±0.13° (Fig. 3), both of which were likely due to the high compliance between the device joint and the biological ankle joint.

While encouraging, these results revealed room for improvement in the performance of the device. Higher torque transmission efficiency could improve tracking and reliability of the controller, as well as allow for reduced motor and battery size. Based on these results we propose the later systematic evaluation method that allows us to quantify and identify the key aspects of the design that could be improved for achieving higher power transmission efficiencies.

Both stroke survivors donned the system independently in an average of ∼7 minutes with no prior experience. According to the participants, the main limitations when donning were that the cables got tangled and the weight distribution of the device caused it to tip over, making it cumbersome. This motivates future design considerations such as including a stand to hold the system in place while donning and using retractable cables that are plugged in once donned, as these may significantly improve the ease of donning.

III. Evaluation of Performance and Power Transmission Efficiency

A. Overview

To characterize the limits of the exoskeleton, we evaluated controller performance with healthy participants walking at different speeds and using a range of assistance profiles. Then, to understand how each aspect of the mechanical design of the exoskeleton contributes to the performance limits, we replayed the ankle kinematics recorded during the walking trials on a custom benchtop dynamometer (Fig. 4A) and measured the flow of power through the system at multiple stages of the transmission.

B. Controller Performance Evaluation

Two unimpaired young adults (1M, 1F) walked with the exoskeleton on an instrumented treadmill (sample rate: 1200 Hz, Bertec, Ohio, USA) while wearing reflective markers. We collected ground reaction forces and motion capture data (sample rate: 200 Hz, Qualisys, Göteborg, Sweden) at two different walking speeds (0.75 and 1.75 m/s) while participants were assisted by individually tuned plantarflexion torque profiles and a constant dorsiflexion angle (15°). Participants first familiarized themselves with the system for ∼5 minutes while plantarflexion was tuned for subjective comfort, followed by a 3-minute walking bout at each

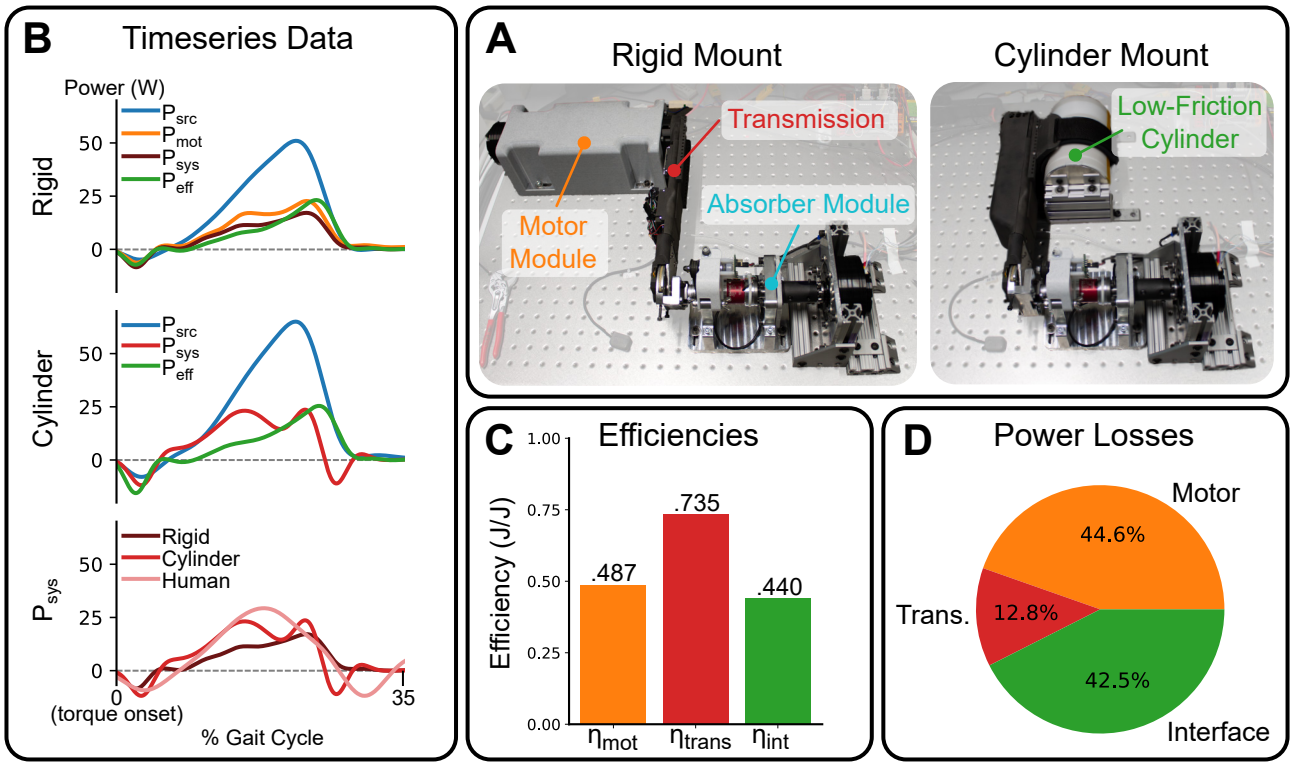

Fig. 4. A) Photos of the custom benchtop dynamometer with the device mounted in both the rigid and cylinder mounting methods. B) Representative segmented plots showing the change in power transmission efficiency at each stage of the transmission for the rigid (top) and the cylinder (middle) mounting conditions, and a comparison of system mechanical powers drawn in each dynamometer condition compared against treadmill walking (bottom). C) Average energy efficiencies of each stage of power transfer of the device. D) RMS power loss at each stage of the device, shown as a fraction of the average total power loss between the battery and the wearer.

walking speed. The peak torque magnitude was set to 25% of typical biological ankle torques, determined from previous data collected on unimpaired young adults and normalized to body weight.

The tracking performance from healthy participants walking at the slower speed (0.75 m/s) showed that peak torque assistance was delayed by an average of 5.21% gait cycle at the slower speed, with an RMS error of 0.13±0.05 N*m/kg, and dorsiflexion angle assistance had an RMS error of 1.6±0.82°. At the higher speed (1.75 m/s), peak torque assistance was delayed by an average of 5.51% gait cycle, with an RMS error of 0.14±0.06 N*m/kg, and dorsiflexion angle assistance had an RMS error of 1.2±0.52°.

From these results, we interpret that the most relevant decline in performance appears from the large delay between peak commanded and measured torques. As with any typical mass-spring-damper system, improving the bandwidth of the device requires increasing the system's stiffness and reducing its weight. In order to reduce the weight and improve the stiffness of the human-robot system, we must identify the dominant sources of compliance and power loss throughout the system so that the next iteration of the device can use smaller, lighter motors while achieving even higher performance. We can identify these inefficiencies by replaying the walking trials on a benchtop dynamometer that allows us to isolate and measure the power flow through multiple stages of the device.

C. Power Transmission Efficiency Analysis

1) Dynamometer Benchtop Setup: The dynamometer used for benchtop characterization consists of a motor module, the exoskeleton transmission, and an absorber module (Fig. 4A). The motor module consists of the exoskeleton actuator motor and a rotary torque sensor (TRS300, Futek, USA), which then attaches to the proximal end of the exoskeleton. The absorber module attaches to the distal end of the exoskeleton and consists of a torque sensor (TFF350, Futek, USA), a hall-effect encoder (AS5600, ams OSRAM, Austria), and an absorber motor (AK10-9 V2.0, Cubemars, China). The motor and absorber modules measure motor power P_{mot} and effective system power P_{eff} as the product of their torques τ_{mot} and τ_{eff} and their angular velocities ω_{mot} and ω_{eff}, respectively. The power of the exoskeleton system P_{sys} is measured as the product of the angular velocity of the exoskeleton encoder ω_{sys} and the more accurate absorber torque sensor τ_{eff}. Meanwhile, voltage V_{src} and current I_{src} are monitored with a voltage divider and an IC current sensor (SEN0098, DFRobot, China), respectively, to measure the electrical source power P_{src} drawn by the motor. All sensing and actuation of the dynamometer are controlled by a Baseline real-time target machine (Speedgoat, Switzerland) running Simulink Real-Time (MathWorks, USA).

2) Test Procedure: In each benchtop trial, we replayed controller commands and biological ankle kinematics from

one of the treadmill walking trials on the benchtop dynamometer. To simulate the wearer's ankle kinematics during walking, we input the measured biological ankle angle as a position command into the absorber motor during plantarflexion assistance and left the absorber motor passive during dorsiflexion assistance. Simultaneously, the exoskeleton actuator was controlled using the same torque and position commands and the same control loops as were used during human subject testing.

We repeated all benchtop tests in two conditions (Fig. 4A). First, we mounted the exoskeleton transmission between the motor and absorber modules, rigidly constraining the device. Second, we replaced the motor torque module with the exoskeleton's usual motor and shank strap, and strapped the shank of the exoskeleton to a low-friction rigid cylinder, allowing the shank interface to deflect naturally. By comparing the power required to follow the commanded torque profile between the rigid benchtop test, the cylinder-mounted benchtop test, and the treadmill walking trials, we were able to separately estimate the power losses due to exoskeleton interface compliance and human soft tissue compliance (Fig. 4C).

3) Data Processing: We replayed both the slow (0.75 m/s) and fast (1.75 m/s) walking bouts of our two unimpaired participants for a total of four trials. Two minutes of walking were replayed for each trial on both the rigid and cylindrical mounting methods. The data from these trials were filtered with a 4th-order low-pass IIR Butterworth with a 15 Hz cutoff frequency, then segmented by stride using the onset of torque assistance.

To compare the effects of interface compliance and human soft tissue compliance separately, we calculated the differences in the power required by the system to follow the commanded torque profile in the rigid and cylinder dynamometer tests as well as in the original walking trials on the treadmill. The difference between P_{sys} (Human) and P_{sys} (Cylinder) provides an estimate of the power lost to deformations of human soft tissue, while the difference between P_{sys} (Cylinder) and P_{sys} (Rigid) estimates the power loss due to deformation of the system interface.

Energy efficiencies (Fig. 4C) were calculated as the ratio of the integral of power through time, averaged across steps and across conditions. Power losses (Fig. 4D) were calculated as the RMS of the difference between power measurements averaged across steps and across conditions.

4) Results & Design Considerations: Comparisons of system power draw between treadmill walking and the Cylinder Mount benchtop test can be used to guide interface design. Our device showed an average of 15 W RMS difference between P_{sys} (Rigid) and P_{sys} (Cylinder), and a 21 W difference between P_{sys} (Cylinder) and P_{sys} (Human). This implies that both interface deformation and human soft tissue play substantial roles in the attenuation of power applied to the wearer.

The measured efficiencies through the system (Fig. 4C) and the power losses (Fig. 4D) may serve as tools to help engineers improve their exoskeleton design. In this study, we find that our motor and interface energy efficiencies are similar (48.7% and 44.0%, respectively). As the motor is higher in the energy flow chain, it likely leads to more net energy loss. However, the power loss is also similar between the motor and interface (44.6% and 42.5%, respectively). So, for this device, future design efforts might be best spent reducing interface compliance to improve controllability. We envision that interface redesign efforts that both distribute load over a wider area on the body and increase interface stiffness will reduce deformation losses in the exoskeleton and lead to improved performance.

IV. Conclusion & Future Work

In this study, we designed a portable, self-donnable, rigid ankle exoskeleton and investigated its potential to assist post-stroke gait during overground, community-based walking. We also presented a systematic method for quantifying power losses at each stage of the transmission to inform future design iterations. Our results showed that the proposed exoskeleton can successfully provide plantarflexion and dorsiflexion assistance during walking, and revealed areas for improvement in the donnability, controller performance, and power transfer efficiency of the proposed ankle exoskeleton. Controller performance and power transfer efficiency were driven by high compliance in the device interface and human soft tissue, highlighting the need to evaluate both energy and power efficiency at multiple stages within a device to maximize device performance while keeping system weight and complexity low. Compared to existing evaluation methods, the proposed method yields a more granular quantification of device performance while characterizing it based on walking data across speeds and individuals. We envision that the iterative design and evaluation paradigm proposed here will serve as a tool for the field to rapidly and systematically improve exoskeletons for real-world use and can be easily replicated.

The first limitation of this work is that our method does not capture the contributions of interaction forces from joint misalignment, which are known to reduce the effective transfer of assistance torque [22]. Second, the benchtop tests used position commands to replay ankle trajectory during plantarflexion assistance, which does not accurately account for the interaction between assistance torque and the wearer's kinematics. This is useful for comparing design changes in a controlled setup, but may not capture how changes to the design change the user's kinematics in response to assistance.

Future work will focus on lowering the interface compliance to increase power transmission efficiency to the user for improved low-level controller performance. Other design improvements will be made based on user feedback to enable independent use at-home.

ACKNOWLEDGMENTS

We would like to thank Ignacio Novillo and Christian Huang for their help developing the exoskeleton, and our clinical research team for their time invested in this study.

REFERENCES

[1] H. S. Jørgensen, H. Nakayama, H. O. Raaschou, and T. S. Olsen, "Recovery of walking function in stroke patients: The copenhagen stroke study," Archives of Physical Medicine and Rehabilitation, vol. 76, no. 1, pp. 27–32, Jan. 1995, publisher: Elsevier. [Online]. Available: https://www.archives-pmr.org/article/S0003-9993(95)80038-7/abstract

[2] D. Rand, J. J. Eng, P.-F. Tang, C. Hung, and J.-S. Jeng, "Daily physical activity and its contribution to the health-related quality of life of ambulatory individuals with chronic stroke," Health and Quality of Life Outcomes, vol. 8, no. 1, p. 80, Aug. 2010. [Online]. Available: https://doi.org/10.1186/1477-7525-8-80

[3] J. L. Moore, E. J. Roth, C. Killian, and T. G. Hornby, "Locomotor Training Improves Daily Stepping Activity and Gait Efficiency in Individuals Poststroke Who Have Reached a "Plateau" in Recovery," Stroke, vol. 41, no. 1, pp. 129–135, Jan. 2010, publisher: American Heart Association. [Online]. Available: https://www.ahajournals.org/doi/10.1161/STROKEAHA.109.563247

[4] T. George Hornby, D. S. Straube, C. R. Kinnaird, C. L. Holleran, A. J. Echauz, K. S. Rodriguez, E. J. Wagner, and E. A. Narducci, "Importance of Specificity, Amount, and Intensity of Locomotor Training to Improve Ambulatory Function in Patients Poststroke," Topics in Stroke Rehabilitation, vol. 18, no. 4, pp. 293–307, July 2011, publisher: Taylor & Francis _eprint: https://doi.org/10.1310/tsr1804-293. [Online]. Available: https://doi.org/10.1310/tsr1804-293

[5] J. Bae, C. Siviy, M. Rouleau, N. Menard, K. O'Donnell, I. Geliana, M. Athanassiu, D. Ryan, C. Bibeau, L. Sloot, P. Kudzia, T. Ellis, L. Awad, and C. J. Walsh, "A Lightweight and Efficient Portable Soft Exosuit for Paretic Ankle Assistance in Walking After Stroke," 2018 IEEE International Conference on Robotics and Automation (ICRA), vol. 00, pp. 2820–2827, 2018.

[6] M. Lee, J. Kim, S. Hyung, J. Lee, K. Seo, Y. J. Park, J. Cho, B.-k. Choi, Y. Shim, and H. Choi, "A Compact Ankle Exoskeleton With a Multiaxis Parallel Linkage Mechanism," IEEE/ASME Transactions on Mechatronics, vol. 26, no. 1, pp. 191–202, 2019.

[7] K. A. Shorter, J. Xia, E. T. Hsiao-Wecksler, W. K. Durfee, and G. F. Kogler, "Technologies for Powered Ankle-Foot Orthotic Systems: Possibilities and Challenges," IEEE/ASME Transactions on Mechatronics, vol. 18, no. 1, pp. 337–347, 2013.

[8] L. N. Awad, J. Bae, K. O'Donnell, S. M. M. D. Rossi, K. Hendron, L. H. Sloot, P. Kudzia, S. Allen, K. G. Holt, T. D. Ellis, and C. J. Walsh, "A soft robotic exosuit improves walking in patients after stroke," Science Translational Medicine, vol. 9, no. 400, p. eaai9084, 2017.

[9] R. W. Nuckols, C.-K. Chang, D. Kim, A. Eckert-Erdheim, D. Orzel, L. Baker, T. Baker, N. C. Wendel, B. Quinlivan, P. Murphy, J. Grupper, J. Villalobos, L. N. Awad, T. D. Ellis, and C. J. Walsh, "Design and evaluation of an independent 4-week, exosuit-assisted, post-stroke community walking program," Annals of the New York Academy of Sciences, vol. 1525, no. 1, pp. 147–159, 2023, _eprint: https://onlinelibrary.wiley.com/doi/pdf/10.1111/nyas.14998. [Online]. Available: https://onlinelibrary.wiley.com/doi/abs/10.1111/nyas.14998

[10] P. Slade, M. J. Kochenderfer, S. L. Delp, and S. H. Collins, "Personalizing exoskeleton assistance while walking in the real world," Nature, vol. 610, no. 7931, pp. 277–282, Oct. 2022, number: 7931 Publisher: Nature Publishing Group. [Online]. Available: https://www.nature.com/articles/s41586-022-05191-1

[11] B. T. Quinlivan, S. Lee, P. Malcolm, D. M. Rossi, M. Grimmer, C. Siviy, N. Karavas, D. Wagner, A. Asbeck, I. Galiana, and C. J. Walsh, "Assistance magnitude versus metabolic cost reductions for a tethered multiarticular soft exosuit," Science Robotics, vol. 2, no. 2, p. eaah4416, Jan. 2017. [Online]. Available: http://robotics.sciencemag.org/content/2/2/eaah4416

[12] J. Zhang, P. Fiers, K. A. Witte, R. W. Jackson, K. L. Poggensee, C. G. Atkeson, and S. H. Collins, "Human-in-the-loop optimization of exoskeleton assistance during walking," Science, vol. 356, no. 6344, pp. 1280–1284, June 2017. [Online]. Available: http://science.sciencemag.org/content/356/6344/1280

[13] D. E. Miller, G. R. Tan, E. M. Farina, A. L. Sheets-Singer, and S. H. Collins, "Characterizing the relationship between peak assistance torque and metabolic cost reduction during running with ankle exoskeletons," Journal of NeuroEngineering and Rehabilitation, vol. 19, no. 1, p. 46, May 2022. [Online]. Available: https://doi.org/10.1186/s12984-022-01023-5

[14] C. Siviy, L. M. Baker, B. T. Quinlivan, F. Porciuncula, K. Swaminathan, L. N. Awad, and C. J. Walsh, "Opportunities and challenges in the development of exoskeletons for locomotor assistance," Nature Biomedical Engineering, vol. 7, no. 4, pp. 456–472, Apr. 2023, number: 4 Publisher: Nature Publishing Group. [Online]. Available: https://www.nature.com/articles/s41551-022-00984-1

[15] L. N. Awad, P. Kudzia, D. A. Revi, T. D. Ellis, and C. J. Walsh, "Walking Faster and Farther With a Soft Robotic Exosuit: Implications for Post-Stroke Gait Assistance and Rehabilitation," IEEE Open Journal of Engineering in Medicine and Biology, vol. 1, pp. 108–115, 2020, conference Name: IEEE Open Journal of Engineering in Medicine and Biology.

[16] L. H. Sloot, L. M. Baker, J. Bae, F. Porciuncula, B. F. Clément, C. Siviy, R. W. Nuckols, T. Baker, R. Sloutsky, D. K. Choe, K. O'Donnell, T. D. Ellis, L. N. Awad, and C. J. Walsh, "Effects of a soft robotic exosuit on the quality and speed of overground walking depends on walking ability after stroke," Journal of NeuroEngineering and Rehabilitation, vol. 20, no. 1, p. 113, Sept. 2023. [Online]. Available: https://doi.org/10.1186/s12984-023-01231-7

[17] G. Orekhov, Y. Fang, C. F. Cuddeback, and Z. F. Lerner, "Usability and performance validation of an ultra-lightweight and versatile untethered robotic ankle exoskeleton," Journal of NeuroEngineering and Rehabilitation, vol. 18, no. 1, p. 163, 2021.

[18] A. T. Asbeck, S. M. D. Rossi, K. G. Holt, and C. J. Walsh, "A biologically inspired soft exosuit for walking assistance," The International Journal of Robotics Research, vol. 34, no. 6, pp. 744–762, 2015.

[19] K. A. Witte, J. Zhang, R. W. Jackson, and S. H. Collins, "Design of two lightweight, high-bandwidth torque-controlled ankle exoskeletons," in 2015 IEEE International Conference on Robotics and Automation (ICRA), May 2015, pp. 1223–1228, iSSN: 1050-4729.

[20] A. Schiele, P. Letier, R. V. Der Linde, and F. V. Der Helm, "Bowden Cable Actuator for Force-Feedback Exoskeletons," in 2006 IEEE/RSJ International Conference on Intelligent Robots and Systems, Oct. 2006, pp. 3599–3604, iSSN: 2153-0866.

[21] J. Zhang, C. C. Cheah, and S. H. Collins, "Experimental comparison of torque control methods on an ankle exoskeleton during human walking," in 2015 IEEE International Conference on Robotics and Automation (ICRA), May 2015, pp. 5584–5589, iSSN: 1050-4729.

[22] R. Mallat, M. Khalil, G. Venture, V. Bonnet, and S. Mohammed, "Human-Exoskeleton Joint Misalignment: A Systematic Review," 2019 Fifth International Conference on Advances in Biomedical Engineering (ICABME), pp. 1–4, 2019.